ADVANCED ELECTRONIC MATERIALS
www.advelectronicmat.de

Catechol-Based Molecular Memory Film for Redox Linked Bioelectronics

Si Wu, Eunkyoung Kim, Chen-yu Chen, Jinyang Li, Eric VanArsdale, Christopher Grieco, Bern Kohler, William E. Bentley, Xiaowen Shi, and Gregory F. Payne**

Redox is emerging as an alternative modality for bio-device communication. In contrast to the more familiar ionic electrical modality: (i) redox involves the flow of electrons through oxidation–reduction reactions; (ii) the aqueous medium is an "insulator" to this electron flow since free electrons do not normally exist in water; and (iii) redox states are intrinsically digital (oxidized and reduced). By exploiting these unique features, a catechol-based molecular memory film is reported. This memory is fabricated by electrochemically grafting catechol to a chitosan–agarose polysaccharide network to generate a redox-active but non-conducting matrix. The redox state of the grafted catechol moieties serves as the 2-state memory. It is shown that these redox states: can be repeatedly switched by diffusible mediators (electron shuttles); can be easily read electrically or optically; are stable for at least 2 h in the absence of energy; are sensitive to biologically relevant oxidizing and reducing contexts; and can be switched enzymatically. This catechol-based molecular memory film is a simple circuit element for redox linked bioelectronics.

A major goal of bioelectronics is to enlist the speed, precision, and computational power of electronics to observe and actuate biological systems. Achieving this goal significantly depends on the communication modality that connects electronic devices to the biological domain. In particular, devices that communicate through biology's ionic electrical modality have been remarkably successful (e.g., electrocardiograms (EKGs) and defibrillators). Recent biological research has demonstrated that redox is an independent biological-signaling modality.[1–8] This redox signaling modality is best understood in host–pathogen immune interactions where an oxidative burst generates a set of reactive species (e.g., reactive oxygen species) that can sometimes be transduced into second messengers (i.e., reactive electrophiles)[4] and ultimately alters biological function through post-translational protein modification (e.g., conversion of protein cysteine residues into disulfide crosslinks).[6] The functions and the coding of information in this redox signaling modality[1] are distinctly different from the information coded in genes or in the action potentials of the ionic electrical modality. Since this redox modality involves the "flow" of electrons through oxidation–reduction reactions, it is accessible to appropriate electrochemical measurement, and this provides new opportunities for bio-device communication.[9–13]

Redox has similarities to the ionic electrical modality, however electrons are the charged species moving in the redox modality. Interestingly, while water is a conductor of ionic currents, it can be considered an "insulator" for the flow of electrons since free electrons do not normally exist in aqueous

S. Wu, Prof. X. Shi
School of Resource and Environmental Science
Hubei International Scientific and Technological Cooperation Base of Sustainable Resource and Energy
Hubei Engineering Center of Natural Polymers-Based Medical Materials
Hubei Biomass-Resource Chemistry and Environmental Biotechnology Key Laboratory
Wuhan University
Wuhan 430079, China
E-mail: shixw@whu.edu.cn

S. Wu, Dr. E. Kim, C.-y. Chen, J. Li, E. VanArsdale, Prof. W. E. Bentley, Prof. G. F. Payne
Institute for Bioscience and Biotechnology Research
University of Maryland
College Park, MD 20742, USA
E-mail: gpayne@umd.edu

The ORCID identification number(s) for the author(s) of this article can be found under https://doi.org/10.1002/aelm.202000452.

Dr. E. Kim, Prof. W. E. Bentley, Prof. G. F. Payne
Robert E. Fischell Institute for Biomedical Devices
University of Maryland
College Park, MD 20742, USA

C.-y. Chen, J. Li, E. VanArsdale, Prof. W. E. Bentley
Fischell Department of Bioengineering and Research
University of Maryland
College Park, MD 20742, USA

Dr. C. Grieco, Prof. B. Kohler
Department of Chemistry and Biochemistry
The Ohio State University
100 West 18th Avenue, Columbus, OH 43210, USA

DOI: 10.1002/aelm.202000452

solution. Thus, biology typically relies on diffusible reductants (e.g., ascorbate and NAD(P)H) and oxidants (e.g., O_2 and reactive oxygen species) to mediate electron "flow" through this redox modality. From a bioelectronics standpoint, both the ionic electrical and redox modalities are accessible to electrode measurement. For the ionic electrical modality, the electrode transduces electrical to ionic currents (often non-Faradaically). For the redox modality, the electrode exchanges electrons with diffusible redox mediators (primarily Faradaically). The "insulating" properties of water and the intrinsic digital nature of redox-states (i.e., oxidized or reduced) suggest that it should be possible to create simple molecular memory devices based on the chemical storage and retrieval of electrons. Technologically, several mechanisms for molecular memory[14,15] are being investigated for bioelectronics.[16–19] Biology also uses various mechanisms: DNA stores information over evolutionary time scales; neuronal circuits emerge during learning to enable individual organisms to form long-term memories; and catecholamine neurotransmitters appear integral to our working memory through mechanisms that are not yet fully understood.[20–22] Here, we report a catechol-based hydrogel memory-film that can be read through orthogonal optical and electrical methods.

Figure 1a shows that our memory-film is fabricated from two polysaccharides, chitosan and agarose, that can form a dual-responsive interpenetrating polymeric network. Due to its unique properties, this chitosan-agarose hydrogel has gained increasing attention in materials science.[23–28] The memory-film is formed by: (i) casting a blend of chitosan (1.5%) and agarose (1%) onto an indium tin oxide (ITO) electrode; and (ii) electrochemically grafting catechol[29] by immersing the hydrogel coated electrode into a catechol solution (10×10^{-3} M catechol in phosphate buffer, pH 7.0) and applying an anodic voltage (1.2 V vs Ag/AgCl; various times up to 30 min) for a controlled charge transfer ($Q_{fab} = \int i dt$). As illustrated in Figure 1a, we adapted the informal nomenclature that is commonly used in the literature to abbreviate chitosan (Chit) and distinguish its two states: the positively charged protonated state (Chit-H^+) and the deprotonated neutral state ($Chit^0$). As illustrated, we suggest that catechol grafting to $Chit^0$ includes Schiff bases and Michael-type adducts[29,30] although this chemistry is complex and may include other grafted moieties (see Supporting Information for additional fabrication details). It is important to note that Michael-type adducts refer to a broad class of chemical linkages that can in some cases be reversible:[31] however, for the quinone–amine Michael-type adducts used here, these linkages are generally believed to be stable.[32,33]

To demonstrate controllable fabrication, we prepared catechol-modified $Chit^0$/agarose films with differing Q_{fab} values and then measured their UV–vis spectra. Figure 1b shows that films prepared without catechol modification ($Q_{fab} = 0$) have little absorbance between 400 and 600 nm, while films with increasing extents of modification (i.e., increasing Q_{fab}) show increasing absorbance. The inset in Figure 1b shows a nearly linear increase in the absorbance at 480 nm (A_{480}) with Q_{fab} with a stronger dependence for films containing chitosan, which is consistent with the greater reactivities of chitosan's amino groups for catechol grafting. In summary, Figure 1b shows that anodic grafting allows $Chit^0$/agarose films to be prepared with controlled amounts of catechol moieties.

Previous studies have shown that catechol-modified hydrogels[34,35] are redox-active but non-conducting, while Figure 1c suggests the grafted catechols possess two stable "memory" states: oxidized (Q) and reduced (QH_2). Figure 1d illustrates that we can "write" to this memory (i.e., switch redox-state) through mediated electrochemistry. To switch this memory-film to the reduced state, we impose a reducing voltage in the presence of the mediator $Ru(NH_3)_6Cl_3$ (Ru^{3+}; $E^0 = -0.2$ V): this induces a reductive redox-cycling in which Ru^{3+} mediates the transfer of electrons from the electrode to the grafted *o*-quinone moieties. To switch this memory-film to the oxidized state, we impose an oxidizing voltage in the presence of the mediator ferrocene dimethanol (Fc; $E^0 = +0.25$ V): this induces an oxidative redox-cycling in which Fc mediates the transfer of electrons from the grafted catechols to the electrode. Importantly, both the Ru^{3+} and Fc mediators can be present in the same solution while the imposed voltage controls if, and which, mediator engages in redox-cycling.[35,36]

Figure 1e shows that we can "read" the memory state non-destructively by measuring the optical absorbance. Specifically, optical (i.e., UV–vis) absorbance is sensitive to chemical structure and we observed that the two redox states have characteristic differences in absorbance. This is illustrated by an experiment in which we fabricated a catechol-$Chit^0$/agarose film ($Q_{fab} = 6$ mC) on the ITO electrode, immersed this film-coated electrode in a solution containing both Ru^{3+} and Fc mediators (0.1×10^{-3} M each), and switched the state several times. To switch the memory-film to its oxidized state (Q) we imposed an oxidizing voltage (+1.2 V, 15 min), and to switch it to its reduced state (QH_2) we imposed a reducing voltage (–0.6 V, 15 min). Figure 1e shows that the oxidized (Q) films repeatedly show higher absorbance compared to the reduced (QH_2) films. The difference spectra (inset in Figure 1e) show an absorption band centered near 480 nm consistent with the molecular interpretation of a Michael-type quinone adduct as suggested in Figure 1a.[37,38]

Spectroelectrochemical analysis was used to characterize the switching-dynamics of our memory-film ($Q_{fab} = 6$ mC). Experimentally, we immersed the film-coated ITO electrode in a mediator solution (0.1×10^{-3} M Fc, 0.1×10^{-3} M Ru^{3+}), imposed oscillating cyclic voltage (CV) inputs, and observed the electrochemical and optical output responses. The leftmost schematic in **Figure 2**a illustrates that at a high scan rate (500 mV s^{-1}), electron transfer at the electrode is expected to be rapid, but the mediators would have little time to diffuse into the film to switch the redox-state of the grafted catechol/*o*-quinone moieties. As expected for this high-scan rate case, Figure 2a shows large output peak currents but small changes in A_{480}. In contrast, the rightmost schematic in Figure 2a illustrates that at low scan rate (5 mV s^{-1}), electron transfer at the electrode is expected to be slower and the mediators would have more time to diffuse deeper into the film to switch the redox-state of a larger fraction of the catechol/*o*-quinone moieties. As expected for this low-scan rate case, the output peak currents are small while a large change in the A_{480} is observed. The middle column in Figure 2a shows that at an intermediate scan rate (50 mV s^{-1}),

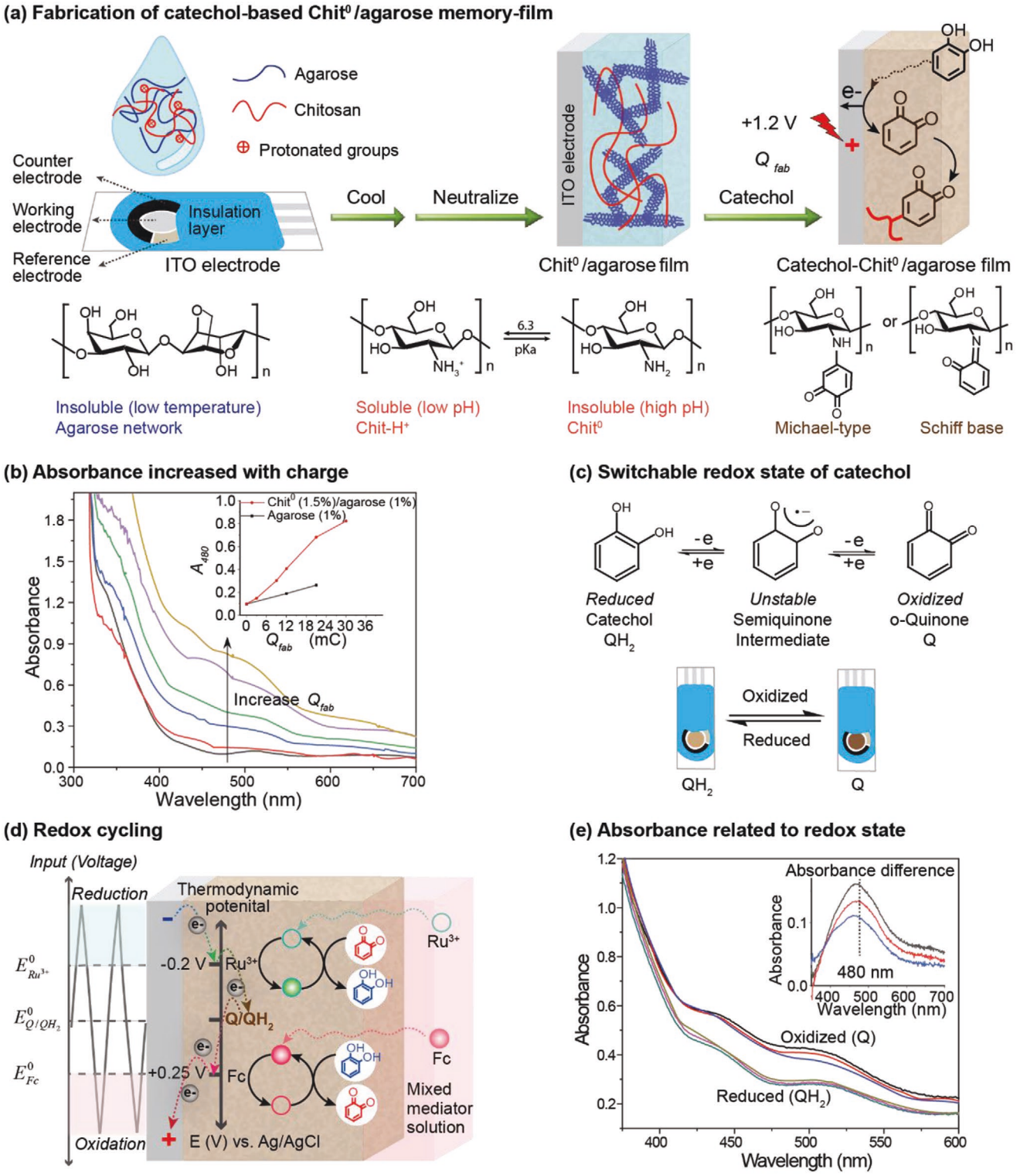

Figure 1. Fabrication and characterization of catechol-Chit^0/agarose memory-film. a) Two stimuli-responsive gel-forming polysaccharides (agarose and chitosan) are cast onto an ITO electrode and catechol moieties are electrochemically grafted using controlled anodic charge (Q_{fab}). b) Catechol grafting is controlled by charge transfer (Q_{fab} = 0, 3, 9, 12, 21, and 30 mC) and is more efficient when chitosan is incorporated into the hydrogel. c) Catechol's two stable redox states (Q and QH_2) serve as the memory states. d) The catechol-Chit^0/agarose memory-film is non-conducting and diffusible mediators are used to switch memory states through thermodynamically controlled redox-cycling reactions. e) The oxidized (Q) films repeatedly show higher absorbance compared to the reduced (QH_2) films and the two memory states can be distinguished by differences in their optical absorbance at 480 nm (A_{480}).

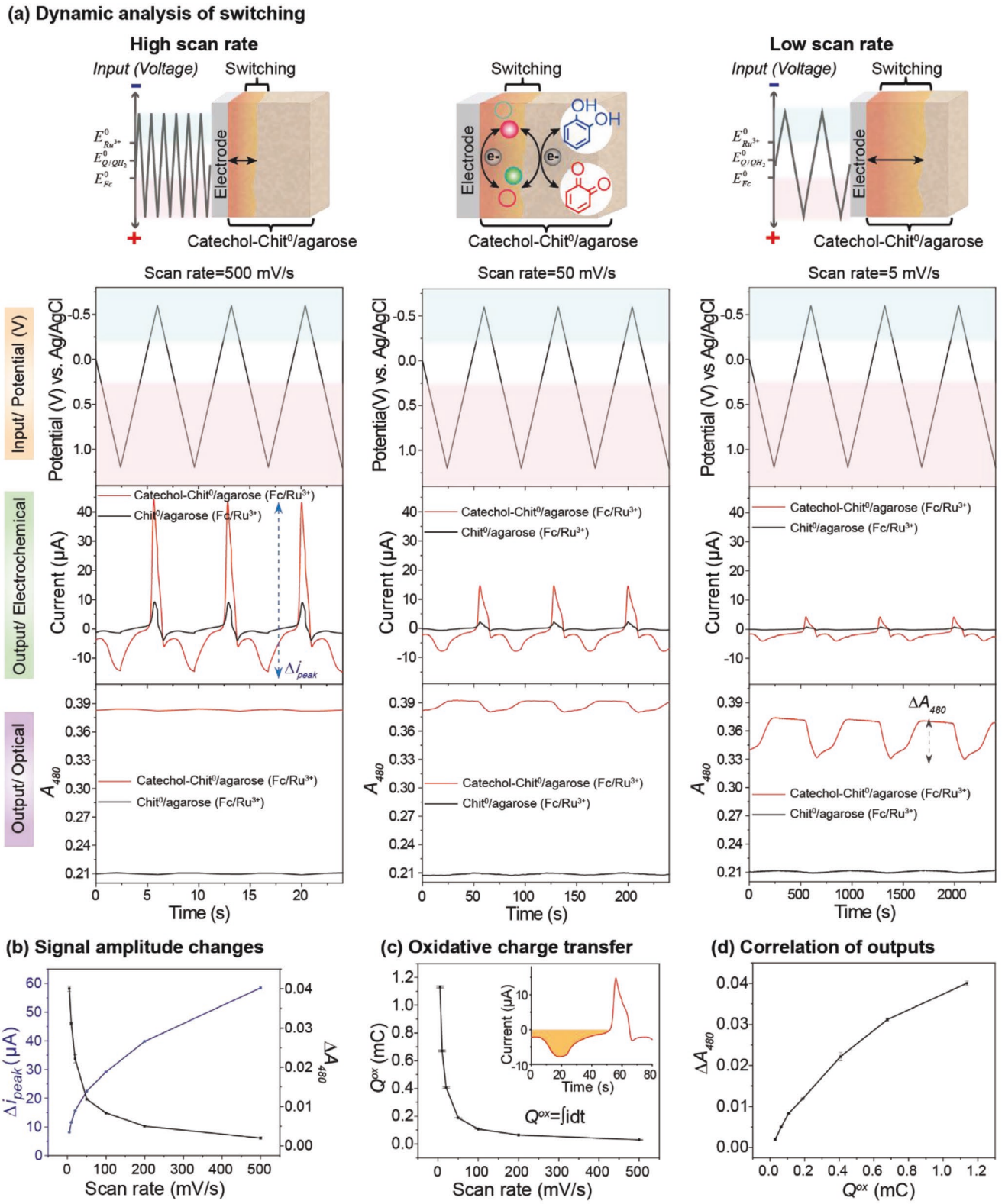

Figure 2. Switching characteristics of catechol-Chit^0/agarose memory-film (Q_{fab} = 6 mC). a) Dynamic spectroelectrochemical analysis shows significantly different optical and electrical output responses (note the large differences in *x*-axis scale). b) Changes in amplitudes for the optical (ΔA_{480}) and current (Δi_{peak}) responses are summarized (note: error bars are small relative to symbol size). c) Output charge transfer during the oxidation segment of the CV cycle (Q^{ox}) decreases with scan rate. d) Correlation between the optical (ΔA_{480}) and electrical (Q^{ox}) output responses.

the observed output currents and optical responses are also intermediate.

To quantify output-responses, Figure 2a shows that we defined amplitudes for: the electrical output as the change in peak current (Δi_{peak}); and the optical output as the change in absorbance (ΔA_{480}). Figure 2b shows a dramatic decrease in optical amplitude with scan rate, while the current amplitude increases monotonically with scan rate. This observation indicates that our memory-film can be read by two modalities that offer markedly different dynamic sensitivities.

To further analyze the electrical output, we integrated the current to calculate the output charge transfer during the oxidation segment of the CV cycle (Q^{ox}) as illustrated in the inset to Figure 2c. When the electrical output is expressed as Q^{ox}, Figure 2c shows a decrease with scan rate that is similar to the decrease observed with the change in optical amplitude. In fact, both ΔA_{480} and Q^{ox} are expected to reflect the total number of redox sites that are switched. Consistent with this expectation, Figure 2d shows a good correlation between the optical (ΔA_{480}) and electrical (Q^{ox}) responses. From a device perspective, these results demonstrate that the independent electrical and optical measurements provide correlated information.

We performed an initial durability test by fabricating a memory-film (Q_{fab} = 15 mC) on a transparent ITO electrode and switching its state multiple times. Experimentally, this film-coated electrode was immersed in a phosphate buffered mediator solution (0.1×10^{-3} M Fc, 0.1×10^{-3} M Ru^{3+}) and an oscillating cyclic voltage (CV) was imposed at 50 mV s^{-1} for 22 cycles. **Figure 3**a shows a steady oscillating output response with large electrical and optical amplitudes (Δi_{peak} = 38 ± 0.95 µA and

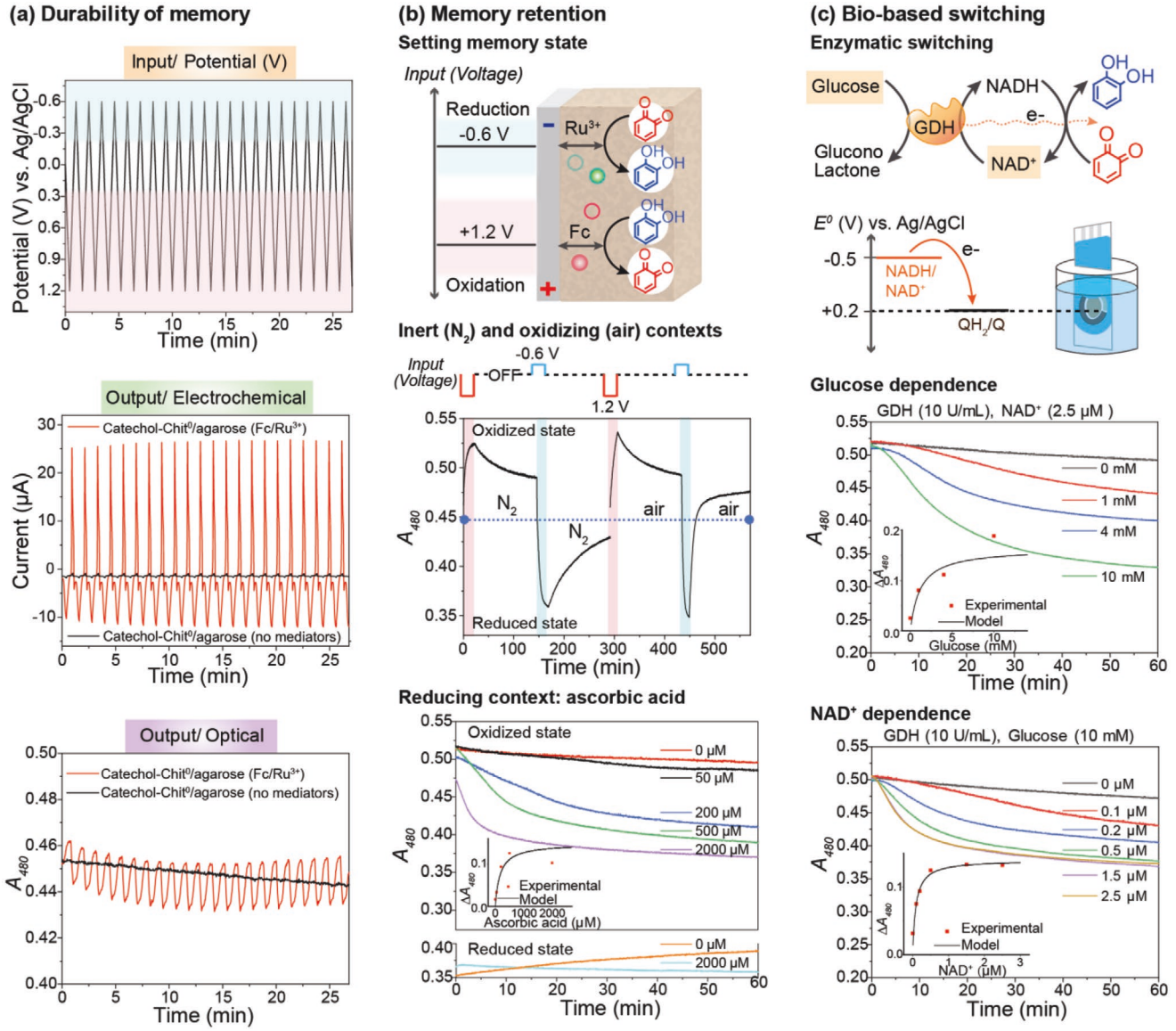

Figure 3. Functional characteristics of the memory-film (Q_{fab} = 15 mC). a) An initial durability test shows repeatable outputs over 22 cycles. b) The memory states are stable for at least 2 h under inert (N_2) conditions but respond to biologically relevant redox contexts (exposure to air or ascorbic acid). c) The memory state can be switched through biological (i.e., enzymatic) mechanisms in a concentration-dependent manner.

$\Delta A_{480} = 0.020 \pm 0.00065$). This result provides initial evidence for the stability of the redox memory mechanism.

There are two important features that are also illustrated in Figure 3a (see Figures S2–S4 of Supporting Information for further discussion). First, the amplitudes observed in Figure 3a are considerably larger than those observed in Figure 2b for the same scan rate (50 mV s^{-1}). This difference occurs because the memory-films in Figure 3a were fabricated with a larger content of redox-active catechols (Q_{fab} = 15 vs 6 mC). Thus, the gain of the memory-film can be controlled during fabrication. Second, the black curves in Figure 3a show results for the same memory-film subjected to the same oscillating voltage inputs but in the absence of the Fc and Ru^{3+} mediators (note: the CV probing was performed first without mediators and then with mediators). The results show that in the absence of mediators, no changes in electrical or optical outputs are observed (i.e., the film's redox-state is not being switched). This result indicates that the memory-films are redox-active but non-conducting (i.e., the imposed voltage is necessary, but not sufficient, for switching). The mediators are essential for switching as they serve as the diffusible electron shuttles that "connect" the electrode to the memory-film, and the mediator's E^0 also serves to "gate" the voltage at which switching occurs.[36]

Next, we examined the ability to retain the redox-memory state and the context-dependence of memory retention. The upper schematic in Figure 3b illustrates that we first set the memory state electrochemically by imposing a constant voltage for 15 min in the presence of the Fc and Ru^{3+} mediators (−0.6 V was imposed to set the reduced state while +1.2 V was imposed to set the oxidized state). After setting the memory states, we tested the stability of these states by shutting off the power and optically observing the change in absorbance over time.

In the first test, we examined stability under inert conditions by bubbling N_2 through the mediator solution before setting the memory state, and then blanketing the solution with N_2 when setting the memory and measuring its stability. The upper plot in Figure 3b shows that we initially set the film to its oxidized state and after shutting off the electrical input observed its absorbance decreased slowly over time. Next, the film was set to its reduced state and after shutting off the electrical input its absorbance was observed to increase slowly. Despite these slow changes, the oxidized and reduced states remain distinguishable over the 2-h test in this inert environment.

In the second test, we examined memory stability under biologically relevant oxidizing conditions (e.g., exposure to air) by transferring the film-coated electrode to an air-saturated mediator solution. The upper plot in Figure 3b shows that the absorbance of the initially oxidized state decreases slowly in the presence of air and this decay is similar to that observed with N_2. In contrast, the absorbance of the initially reduced state increases sharply upon exposure to air which is consistent with the ability of O_2 to accept electrons from the reduced catechol moieties.[39]

In the third test, we examined the memory stability under biologically relevant reducing conditions (e.g., ascorbic acid solution) by electrochemically setting the memory state, and then immediately transferring the film-coated electrodes to solutions containing ascorbic acid (note: N_2 was bubbled through the ascorbic acid solutions prior to measurement and an N_2 blanket was used during measurement). The bottom curve in Figure 3b shows that the absorbance of the initially reduced state is stabilized by ascorbic acid, while the absorbance of the initially oxidized state decreases in the presence of ascorbic acid in a manner that can be described by a saturation model (see inset of Figure 3b and details of Figure S5a in Supporting Information). These observations are consistent with the ability of the oxidized *o*-quinone moieties to accept electrons from the biological reducing agent ascorbic acid.[39]

As suggested in Figure 3b, an important feature of catechol-based molecular memory-film is its ability to be switched through biologically relevant mechanisms (i.e., biological oxidants/reductants can write to this memory).[35] Such redox-based biological communication is further illustrated by the experiment in Figure 3c which shows enzyme-catalyzed writing-to (i.e., switching-of) our memory-film. As illustrated, glucose dehydrogenase (GDH) was used to catalyze the transfer of electrons from glucose to NAD^+ while the subsequent redox-cycling of NADH serves to switch the film's redox-state to its reduced (QH_2) form.[11] Experimentally, we first electrochemically set the memory to its oxidized (Q) state as described in Figure 3b, and then immersed the film-coated electrode into solutions containing GDH, NAD^+, and glucose. The two plots in Figure 3c show the absorbance decreased in a glucose-dependent and NAD^+-dependent manner. The insets summarize the experimental results and their fits to a saturation models (see Figure S5 in Supporting Information). These plots demonstrate that the catechol memory can receive and record biologically relevant information (i.e., the presence and levels of glucose or NAD^+).

In conclusion, we report a redox-based molecular memory-film that is easy to fabricate and employs an operationally simple mechanism. From a memory perspective, the film appears durable and can be repeatedly switched, while the memory is stable for at least 2 h without the need for energy. From a measurement perspective, the memory can be observed through orthogonal optical and electrical modalities that are correlated but offer different sensitivities and dynamics. From a bioelectronics perspective, the memory can respond to biologically relevant redox contexts and engage biological redox-activities (e.g., enzyme-catalyzed redox reactions) through thermodynamically controlled electron transfer reactions. Overall, this work further extends the functional possibilities of catechol-based materials that are of increasing interest in biology (e.g., melanin[40–47]) and technology (e.g., polydopamine[48–51]).

Supporting Information

Supporting Information is available from the Wiley Online Library or from the author.

Acknowledgements

This work was supported by the United States National Science Foundation (ECCS-1807604, CBET-1932963, CBET-1805274) and Defense Threat Reduction Agency (HDTRA-11910021), and by National Natural Science Foundation of China (51373124), Fundamental Research Funds

for the Central Universities (2042016kf0145), and the China Scholarship Council.

Conflict of Interest

The authors declare no conflict of interest.

Keywords

catechol, molecular memories, polysaccharides, redox linked bioelectronics, spectroelectrochemistry

Received: April 29, 2020
Revised: June 11, 2020
Published online:

[1] D. P. Jones, H. Sies, *Antioxid. Redox Signaling* **2015**, *23*, 734.
[2] Y.-M. Go, D. P. Jones, *J. Biol. Chem.* **2013**, *288*, 26512.
[3] M. Kemp, Y.-M. Go, D. P. Jones, *Free Radical Biol. Med.* **2008**, *44*, 921.
[4] S. Parvez, M. J. C. Long, J. R. Poganik, Y. Aye, *Chem. Rev.* **2019**, *119*, 4464.
[5] J. D. Matthews, A. R. Reedy, H. Wu, B. H. Hinrichs, T. M. Darby, C. Addis, B. S. Robinson, Y.-M. Go, D. P. Jones, R. M. Jones, A. S. Neish, *Redox Biol.* **2019**, *20*, 526.
[6] S. García-Santamarina, S. Boronat, E. Hidalgo, *Biochemistry* **2014**, *53*, 2560.
[7] M. Schieber, N. S. Chandel, *Curr. Biol.* **2014**, *24*, R453.
[8] A. R. Timme-Laragy, M. E. Hahn, J. M. Hansen, A. Rastogi, M. A. Roy, *Semin. Cell Dev. Biol.* **2018**, *80*, 17.
[9] E. Kim, J. Li, M. Kang, D. L. Kelly, S. Chen, A. Napolitano, L. Panzella, X. Shi, K. Yan, S. Wu, J. Shen, W. E. Bentley, G. F. Payne, *Proc. IEEE* **2019**, *107*, 1402.
[10] T. Tschirhart, E. Kim, R. McKay, H. Ueda, H.-C. Wu, A. E. Pottash, A. Zargar, A. Negrete, J. Shiloach, G. F. Payne, W. E. Bentley, *Nat. Commun.* **2017**, *8*, 14030.
[11] E. Kim, Y. Liu, W. E. Bentley, G. F. Payne, *Adv. Funct. Mater.* **2012**, *22*, 1409.
[12] T. E. Winkler, R. Dietrich, E. Kim, H. Ben-Yoav, D. L. Kelly, G. F. Payne, R. Ghodssi, *Electrochem. Commun.* **2017**, *79*, 33.
[13] W. Shang, Y. Liu, E. Kim, C. Y. Tsao, G. F. Payne, W. E. Bentley, *Lab Chip* **2018**, *18*, 3578.
[14] W. P. Lin, S. J. Liu, T. Gong, Q. Zhao, W. Huang, *Adv. Mater.* **2014**, *26*, 570.
[15] I. Valov, *Semicond. Sci. Technol.* **2017**, *32*, 093006.
[16] Y. Liu, M. Pharr, G. A. Salvatore, *ACS Nano* **2017**, *11*, 9614.
[17] D. P. Dubal, N. R. Chodankar, D. H. Kim, P. Gomez-Romero, *Chem. Soc. Rev.* **2018**, *47*, 2065.
[18] Z. Wang, H. Wu, G. W. Burr, C. S. Hwang, K. L. Wang, Q. Xia, J. J. Yang, *Nat. Rev. Mater.* **2020**, *5*, 173.
[19] M. D. Manrique-Juárez, S. Rat, L. Salmon, G. Molnár, C. M. Quintero, L. Nicu, H. J. Shepherd, A. Bousseksou, *Coord. Chem. Rev.* **2016**, *308*, 395.
[20] R. Cools, S. E. Gibbs, A. Miyakawa, W. Jagust, M. D'Esposito, *J. Neurosci.* **2008**, *28*, 1208.
[21] R. Cools, M. D'Esposito, *Biol. Psychiatry* **2011**, *69*, e113.
[22] P. O. Jenkins, M. A. Mehta, D. J. Sharp, *Brain* **2016**, *139*, 2345.
[23] S. Wu, K. Yan, Y. Zhao, C. C. Tsai, J. Shen, W. E. Bentley, Y. Chen, H. Deng, Y. Du, G. F. Payne, X. Shi, *Adv. Funct. Mater.* **2018**, *28*, 1.
[24] S. Wu, W. Wang, K. Yan, F. Ding, X. Shi, H. Deng, Y. Du, *Carbohydr. Polym.* **2018**, *186*, 236.
[25] K. Yan, Y. Xiong, S. Wu, W. E. Bentley, H. Deng, Y. Du, G. F. Payne, X. W. Shi, *ACS Appl. Mater. Interfaces* **2016**, *8*, 19780.
[26] K. Yan, F. Xu, S. Li, Y. Li, Y. Chen, D. Wang, *Colloids Surf., B* **2020**, *190*, 110907.
[27] E. R. Cross, *SN Appl. Sci.* **2020**, *2*, 397.
[28] B. C. Zarket, S. R. Raghavan, *Nat. Commun.* **2017**, *8*, 193.
[29] L.-Q. Wu, M. K. McDermott, C. Zhu, R. Ghodssi, G. F. Payne, *Adv. Funct. Mater.* **2006**, *16*, 1967.
[30] L.-Q. Wu, R. Ghodssi, Y. A. Elabd, G. F. Payne, *Adv. Funct. Mater.* **2005**, *15*, 189.
[31] W. Huang, X. Wu, X. Gao, Y. Yu, H. Lei, Z. Zhu, Y. Shi, Y. Chen, M. Qin, W. Wang, Y. Cao, *Nat. Chem.* **2019**, *11*, 310.
[32] S. Bittner, *Amino Acids* **2006**, *30*, 205.
[33] J. H. Ryu, S. Hong, H. Lee, *Acta Biomater.* **2015**, *27*, 101.
[34] E. Kim, Y. Liu, X. W. Shi, X. Yang, W. E. Bentley, G. F. Payne, *Adv. Funct. Mater.* **2010**, *20*, 2683.
[35] S. Wu, E. Kim, J. Li, W. E. Bentley, X.-W. Shi, G. F. Payne, *ACS Appl. Electron. Mater.* **2019**, *1*, 1337.
[36] E. Kim, W. T. Leverage, Y. Liu, I. M. White, W. E. Bentley, G. F. Payne, *Analyst* **2014**, *139*, 32.
[37] C. Chen, D. R. Thakker, *J. Pharmacol. Exp. Ther.* **2002**, *300*, 417.
[38] C. Grieco, J. M. Empey, F. R. Kohl, B. Kohler, *Faraday Discuss.* **2019**, *216*, 520.
[39] H. Liu, X. Qu, E. Kim, M. Lei, K. Dai, X. Tan, M. Xu, J. Li, Y. Liu, X. Shi, P. Li, G. F. Payne, C. Liu, *Biomaterials* **2018**, *162*, 109.
[40] R. P. Gajula, S. Gaddameedhi, *Front. Physiol.* **2015**, *6*, 842.
[41] M. d'Ischia, A. Napolitano, A. Pezzella, P. Meredith, M. J. Buehler, *Angew. Chem., Int. Ed.* **2019**, *59*, 2.
[42] M. d'Ischia, K. Wakamatsu, F. Cicoira, E. Di Mauro, J. C. Garcia-Borron, S. Commo, I. Galván, G. Ghanem, K. Kenzo, P. Meredith, A. Pezzella, C. Santato, T. Sarna, J. D. Simon, L. Zecca, F. A. Zucca, A. Napolitano, S. Ito, *Pigm. Cell Melanoma Res.* **2015**, *28*, 520.
[43] M. Sheliakina, A. B. Mostert, P. Meredith, *Mater. Horiz.* **2018**, *5*, 256.
[44] A. B. Mostert, B. J. Powell, F. L. Pratt, G. R. Hanson, T. Sarna, I. R. Gentle, P. Meredith, *Proc. Natl. Acad. Sci. U. S. A.* **2012**, *109*, 8943.
[45] Y. J. Kim, A. Khetan, W. Wu, S. E. Chun, V. Viswanathan, J. F. Whitacre, C. J. Bettinger, *Adv. Mater.* **2016**, *28*, 3173.
[46] X. Zhou, N. C. McCallum, Z. Hu, W. Cao, K. Gnanasekaran, Y. Feng, J. F. Stoddart, Z. Wang, N. C. Gianneschi, *ACS Nano* **2019**, *13*, 10980.
[47] A. Lampel, S. A. McPhee, H. A. Park, G. G. Scott, S. Humagain, D. R. Hekstra, B. Yoo, P. W. J. M. Frederix, T. De Li, R. R. Abzalimov, S. G. Greenbaum, T. Tuttle, C. Hu, C. J. Bettinger, R. V. Ulijn, *Science.* **2017**, *356*, 1064.
[48] C. J. Higginson, K. G. Malollari, Y. Xu, A. V. Kelleghan, N. G. Ricapito, P. B. Messersmith, *Angew. Chem., Int. Ed.* **2019**, *131*, 12399.
[49] P. Delparastan, K. G. Malollari, H. Lee, P. B. Messersmith, *Angew. Chem., Int. Ed.* **2019**, *131*, 1089.
[50] K. Ni, H. Lu, C. Wang, K. C. L. Black, D. Wei, Y. Ren, P. B. Messersmith, *Biotechnol. Bioeng.* **2012**, *109*, 2970.
[51] H. A. Lee, E. Park, H. Lee, *Adv. Mater.* **2020**, 1907505.

